SF2A 2013
L. Cambrésy, F. Martins, E. Nuss and A. Palacios (eds)

EFFECT OF INTERNAL GRAVITY WAVES ON THE TRANSPORT OF ANGULAR MOMENTUM DURING THE PMS

T. Decressin[1], C. Charbonnel[1,2], L. Amard[3], A. Palacios[3] and S. Talon[4]

Abstract. In stellar interior rotation profile can be changed by stellar contraction, meridional circulation, shear turbulence and internal gravity waves. These waves are generated at the edge of the convective zones and propagate inside the radiative zone where they damped by thermal diffusivity and viscosity in corotation resonance. The differential damping between prograde and retrograde let its imprint on the rotation profile along with other hydrodynamic transport processes. This interplay will be discussed for low-mass stars along the PMS.

Keywords: stars: evolution – stars: interiors – stars: low-mass – stars: rotation

1 Introduction

We present pre-main sequence (hereafter PMS) models for low-mass rotating stars (0.6 to 2.0 $M_{\odot}$) at solar metallicity computed with the stellar evolution code STAREVOL (see Siess et al. 2000; Palacios et al. 2003; Decressin et al. 2009; Lagarde et al. 2012, for more details). Initially we assume a solid-body law for rotation with a surface velocity equals to 5% of the critical velocity when the radiative core appears. Our models reach surface velocity around 50-80 km.s^{-1} on the zero age main sequence (hereafter ZAMS). We follow the formalism developed by Zahn (1992) and Mathis & Zahn (2004) for the transport of angular momentum by meridional circulation, shear turbulence and internal gravity waves (hereafter IGW). In these computation we assume no loss of angular momentum by radiative winds during the PMS (see Charbonnel et al. 2013, for more details). Such models with a self-consistent treatment of rotation evolution can be used to understand the observations of surface velocity in open cluster stars (Irwin & Bouvier 2009; Gallet & Bouvier 2013).

2 IGW excitation

In this work we follow the formalism developed by Talon & Charbonnel (2005) for the excitation and the transport of angular momentum by IGW by the convective envelope and the convective core when present. Both prograde and retrograde waves are taken into account and the excitation is computed at each time-step to account for the structural changes along the PMS. Once emitted a wave travels through the radiative interior and it mainly damps near its critical layer (*i.e.*, the location where the local relative frequency of a given wave to the rotational frequency of the fluid tends to zero, see also Alvan et al. 2013) where they will extract or deposit angular momentum. As prograde and retrograde waves are damped in different region, a net transport of angular momentum happens.

The excitation by Reynolds stress and the buoyancy in the bulk of convective regions is computed following Goldreich et al. (1994) and Kumar & Quataert (1997). We multiply the resulting luminosity by a factor 2 to account the recent results by Lecoanet & Quataert (2012). The obtained spectra for IGW are still uncertain as we include neither the generation by convective overshooting plumes (Garcia Lopez & Spruit 1991) nor the effects of Coriolis force (Mathis 2009).

[1] Observatoire de Genve 51, chemin des Maillettes CH-1290 Sauverny, Switzerland
[2] IRAP, CNRS UMR 5277, Universit de Toulouse, 14 Av. E. Belin, 31400 Toulouse, France
[3] LUPM, Universit Montpellier II, CNRS, UMR 5299, Place E. Bataillon, 34095 Montpellier, France
[4] Calcul Qubec, Universit de Montral (DGTIC), C.P. 6128, succ. Centre-ville, Montral (Qubec) H3C 3J7, Canada

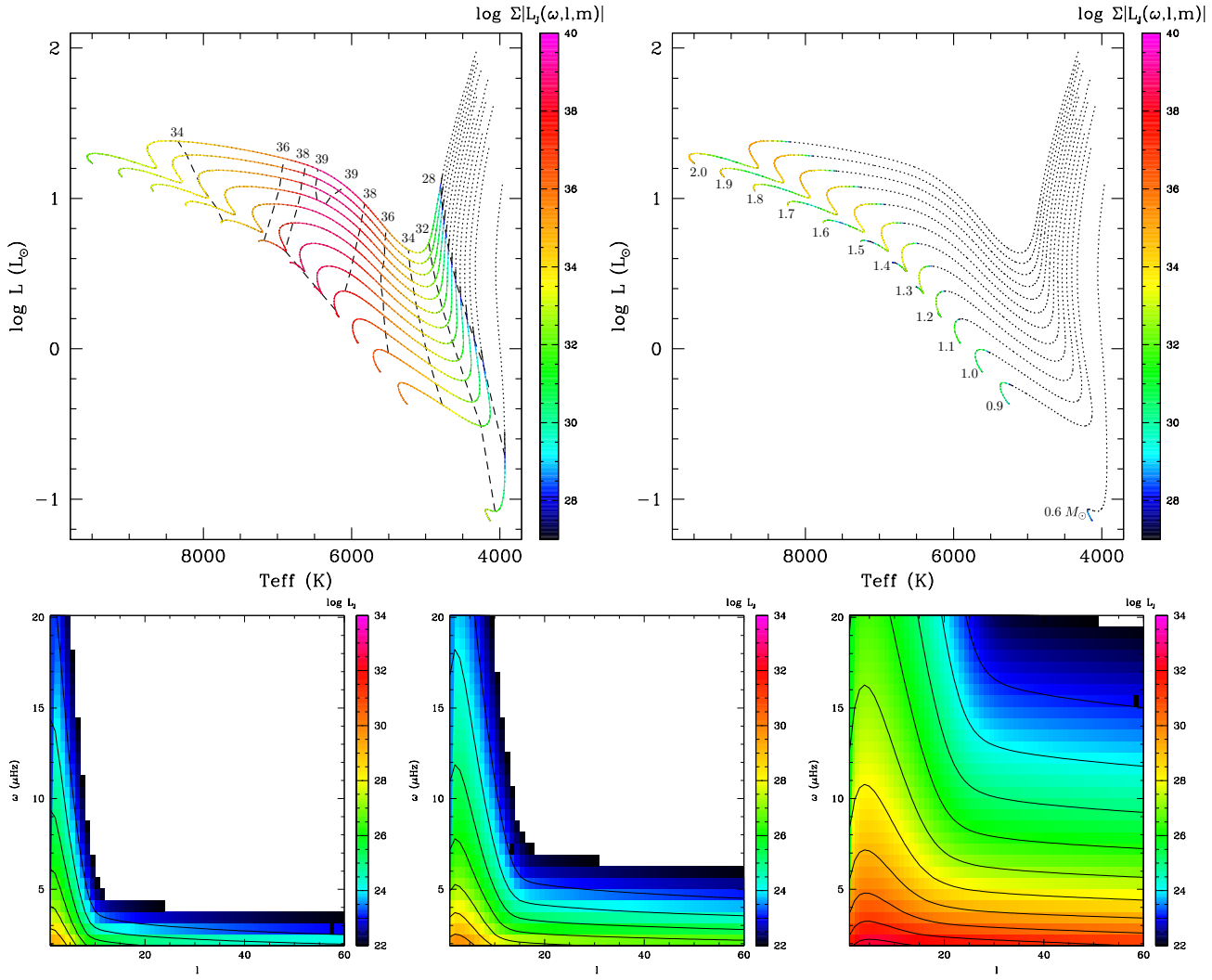

Fig. 1. *Top panels*: tracks along the PMS for 0.6 to 2.0 $M_\odot$ stars at solar metallicity with the colours indicate the total luminosity of IGW excited by the convective envelope (left) and the convective core (right). Dotted lines indicate when the stars are fully convective or have no convective core. *Bottom panels*: spectra of the IGW emitted by the convective envelope of a 1 $M_\odot$ with solar metallicity at 5.8, 14 and 35 Myr.

Figure 1 shows the computed total excitation luminosity of IGW for all our PMS models both from the convective envelope and convective core. The waves luminosity from the convective envelope rises sharply once a radiative core appears at the end of the vertical Hayashi line and present a maximum around $T_{\rm eff} \simeq 6200$ K. For stars heavier than 1.3-1.4 $M_\odot$ the luminosity decreases when the stars approach the ZAMS as a result of the drop in size (both in radius and mass coordinates) of the convective envelope. On the other side the waves emitted by the convective core at the end of the PMS are always negligible for stars below 1.3-1.4 $M_\odot$, and they becomes only dominant when those heavier stars approach the ZAMS.

The bottom panels of Fig. 1 show the development of the IGW luminosity spectra for a 1 $M_\odot$ star along the PMS reflecting the evolving properties of the convective envelope during the PMS. As the star cools, more waves are efficiently generated while these with low internal frequency and low number l remains the dominant ones (see also Talon & Charbonnel 2003).

3 Effects of IGW during pre-main sequence

The IGW has a strong effects on the transport of angular momentum in radiative interior. In the absence of IGW, angular momentum is mainly advected by meridional circulation which shows only one or two main loops

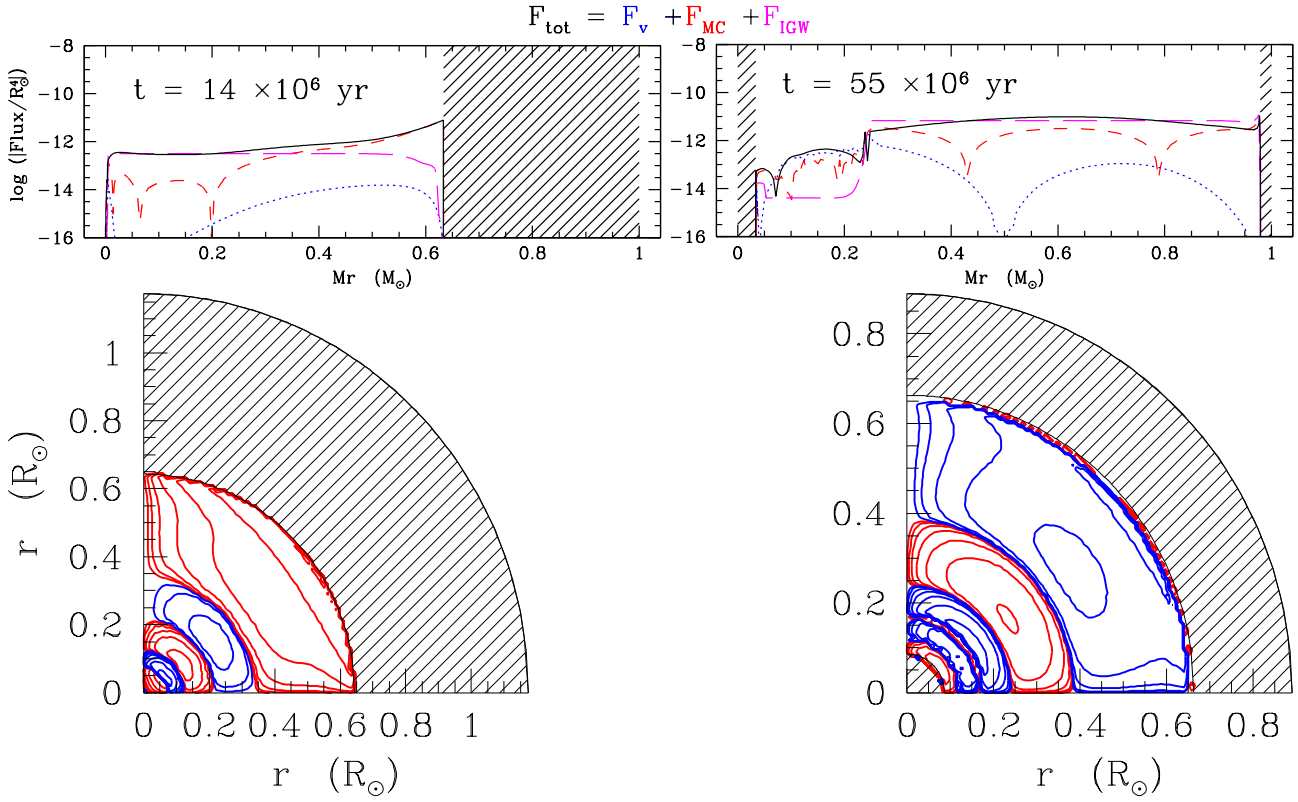

Fig. 2. *Top panels*: Decomposition of the total flux of angular momentum (solid black) into meridional circulation (short-dashed red), shear turbulence (dotted blue), and IGW (long-dashed magenta) in the 1 $M_\odot$, $Z_\odot$, models. The profiles are shown at 14 and 55 Myr. Shaded areas correspond to convective regions. *Bottom panels*: reconstruction of the meridional circulation inside the same star.

(see Decressin et al. 2009; Charbonnel et al. 2013). As shown in Fig. 2 for a 1 $M_\odot$ model, IGW induce a different behaviour as they dominate the angular momentum transport by conveying angular momentum directly from the radiative interior where they damped toward the convective envelope. The meridional circulation and the shear only dominates the transport in the inner radiative interior where IGW are efficiently damped (see top right panel of Fig. 2 below 0.25 $M_\odot$). As a results the angular velocity profile shows a peak in the radiative interior, that in turn will induce numerous loops of meridional circulation as illustrated in the bottom panels of Fig. 2. This multi-loops pattern will persist as long as IGW stay the dominant transport mechanism (see Talon & Charbonnel 2005 and Mathis et al, subm., for a description on the main sequence).

Fig. 3 shows how the rotation profile changes with the addition of IGW at the ZAMS for models with an initial mass from 0.6 to 2.0 $M_\odot$. For stars below 1.4 $M_\odot$, IGW induces a slowly rotating core and a peak in angular velocity, whereas only a monotonous differential rotation is obtained if only meridional circulation and shear turbulence is taken into account. This peculiar shape in peak results (1) from the overall contraction of the star that produces the negative gradient of angular velocity in the outer part of the radiative envelope and (2) from the extraction of angular momentum by IGW in the centre.

For heavier stars than 1.4 $M_\odot$, similarly a peak in the profile angular momentum formed when the waves from the convective envelope are efficiently generated (see Fig. 1). However when reaching the ZAMS, IGW from the core dominates and transport angular momentum inwards. Thus they tends to accelerate the core and the differences with models without IGW becomes smaller (see Charbonnel et al. 2013).

We acknowledge financial support from the Swiss National Science Foundation (FNS), from the French Programme National de Physique Stellaire (PNPS) of CNRS/INSU, and from the Agence Nationale de la Recherche (ANR) for the project TOUPIES (Towards Understanding the sPIn Evolution of Stars).

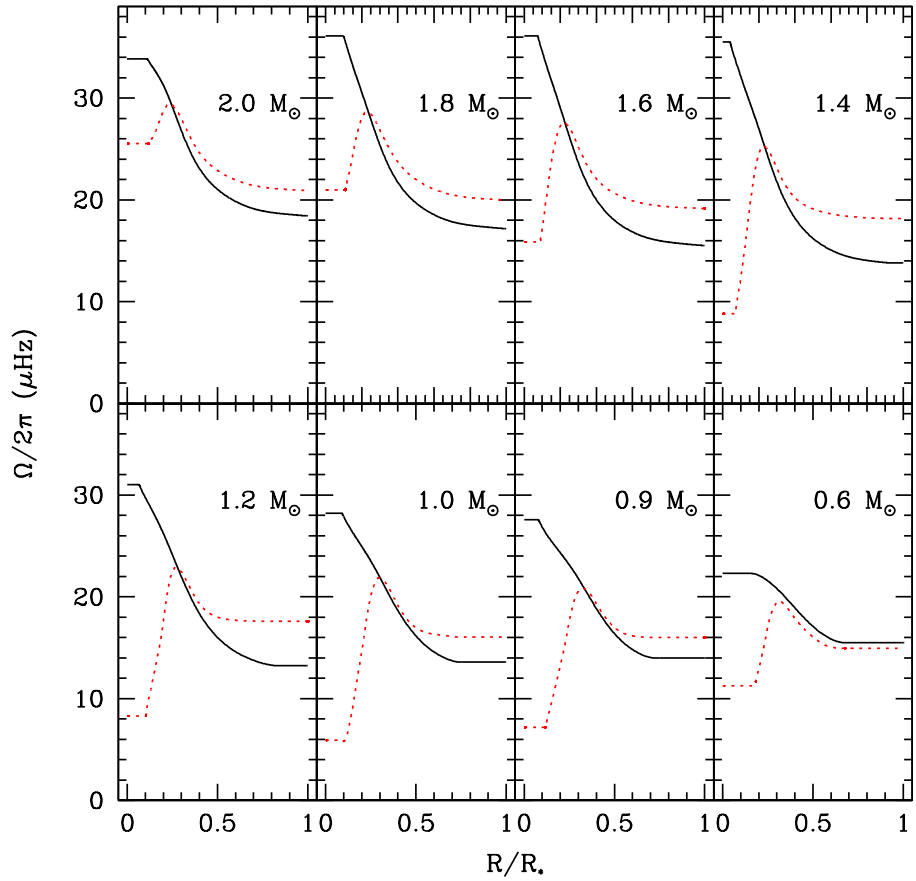

Fig. 3. Internal angular velocity profile for stars from 0.6 to 2.0 $M_{\odot}$, $Z_{\odot}$, at the ZAMS with taking into account the effect of IGW (dashed lines) and without them (full lines).

References

Alvan, L., Mathis, S., & Decressin, T. 2013, A&A, 552, 121

Charbonnel, C., Decressin, T., Amard, L., Palacios, A., & Talon, S. 2013, A&A, 554, 40

Decressin, T., Mathis, S., Palacios, A., et al. 2009, A&A, 495, 271

Gallet, F. & Bouvier, J. 2013, A&A, 556, A36

Garcia Lopez, R. J. & Spruit, H. C. 1991, ApJ, 377, 268

Goldreich, P., Murray, N., & Kumar, P. 1994, ApJ, 424, 466

Irwin, J. & Bouvier, J. 2009, in IAU Symposium, Vol. 258, IAU Symposium, ed. E. E. Mamajek, D. R. Soderblom, & R. F. G. Wyse, 363–374

Kumar, P. & Quataert, E. J. 1997, ApJ, 475, L143

Lagarde, N., Decressin, T., Charbonnel, C., et al. 2012, A&A, 543, A108

Lecoanet, D. & Quataert, E. 2012, ArXiv e-prints

Mathis, S. 2009, A&A, 506, 811

Mathis, S. & Zahn, J.-P. 2004, A&A, 425, 229

Palacios, A., Talon, S., Charbonnel, C., & Forestini, M. 2003, A&A, 399, 603

Siess, L., Dufour, E., & Forestini, M. 2000, A&A, 358, 593

Talon, S. & Charbonnel, C. 2003, A&A, 405, 1025

Talon, S. & Charbonnel, C. 2005, A&A, 440, 981

Zahn, J.-P. 1992, A&A, 265, 115